Medical Physics
The International Journal of Medical Physics Research and Practice

The Octavius1500 2D ion chamber array and its associated phantoms: Dosimetric characterization of a new prototype

Ann Van Esch, Katarzyna Basta, Marie Evrard, Michel Ghislain, Francois Sergent, and Dominique P. Huyskens

Citation: Medical Physics **41**, 091708 (2014); doi: 10.1118/1.4892178
View online: http://dx.doi.org/10.1118/1.4892178
View Table of Contents: http://scitation.aip.org/content/aapm/journal/medphys/41/9?ver=pdfcov
Published by the American Association of Physicists in Medicine

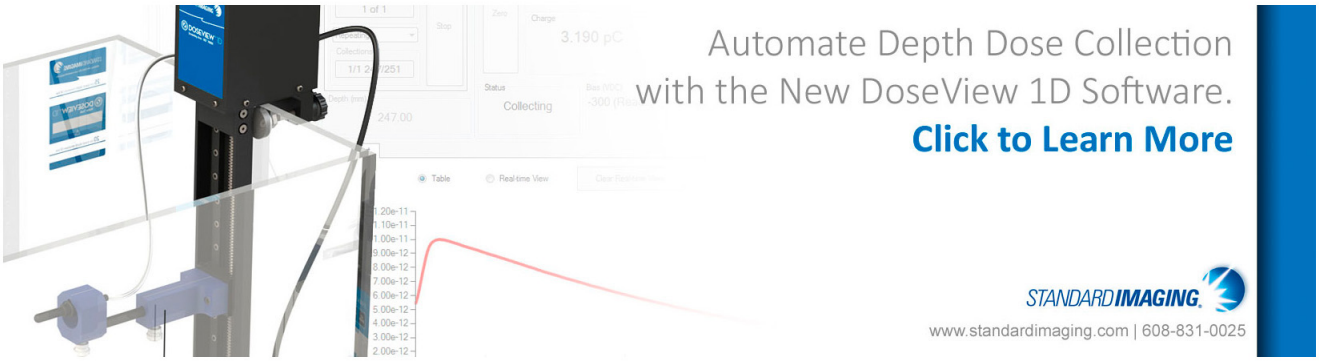

The Octavius1500 2D ion chamber array and its associated phantoms: Dosimetric characterization of a new prototype

Ann Van Esch[a)]
7Sigma, QA-team in radiotherapy physics, Kasteeldreef 2, 3150 Tildonk, Belgium; Radiotherapy Association, Centre Hospitalier Mouscron – Ste Elisabeth Namur, 7700 Mouscron – 5000 Namur, Belgium

Katarzyna Basta, Marie Evrard, Michel Ghislain, and Francois Sergent
Radiotherapy Association, Centre Hospitalier Mouscron – Ste Elisabeth Namur, 7700 Mouscron – 5000 Namur, Belgium

Dominique P. Huyskens
7Sigma, QA-team in radiotherapy physics, Kasteeldreef 2, 3150 Tildonk, Belgium; Radiotherapy Association, Centre Hospitalier Mouscron – Ste Elisabeth Namur, 7700 Mouscron – 5000 Namur, Belgium

(Received 22 March 2014; revised 16 July 2014; accepted for publication 19 July 2014; published 25 August 2014)

Purpose: The purpose of the study is to characterize the prototype of the new Octavius1500 (PTW, Freiburg, Germany) 2D ion chamber array, covering its use in different phantom setups, from the most basic solid water sandwich setup to the more complex cylindrical Octavius® 4D (Oct4D) (PTW) phantom/detector combination. The new detector houses nearly twice the amount of ion chambers as its predecessors (Seven29 and Octavius729), thereby tackling one of the most important limitations of ion chamber (or diode) arrays, namely the limited detector density. The 0.06 cm^3 cubic ion chambers are now arranged in a checkerboard pattern, leaving no lines (neither longitudinally nor laterally) without detectors.

Methods: All measurements were performed on a dual energy (6 MV and 18 MV) iX Clinac (Varian Medical Systems, Palo Alto, CA) and all calculations were done in the Eclipse treatment planning system (Varian) with the Anisotropic Analytical Algorithm. First, the basic characteristics of the 2D array, such as measurement stability, dose rate dependence and dose linearity were investigated in the solid water sandwich setup. Second, the directional dependence was assessed to allow the evaluation of the new Octavius2D phantom ($Oct2D^{1500}$) for planar verification measurements of composite plans. Third, measurements were performed in the Oct4D phantom to evaluate the impact of the increased detector density on the accuracy of the volumetric dose reconstruction.

Results: While showing equally good dose linearity and dose rate independence, the Octavius1500 outperforms the previous models because of its instantaneous measurement stability and its twofold active area coverage. Orthogonal field-by-field measurements immediately benefit from the increased detector density. The 3.9 cm wide compensation cavity in the new $Oct2D^{1500}$ phantom prototype adequately corrects for directional dependence from the rear, resulting in good agreement within the target dose. Discrepancies may arise towards the sides of the array because of uncompensated lateral beam incidence. The beneficial impact of the detector density is most prominent in the Oct4D system, for which the average pass rate (PR) is now nearly 100% (99.31 ± 0.37) when using gamma criteria of 2%G,2 mm (10% dose threshold). In search of gamma analysis criteria that are not too lenient to detect possibly relevant deviations, the authors conclude that for our radiotherapy environment, the authors choose to adopt 3%L,3 mm PR97% (threshold 10%) criteria for the $Oct2D^{1500}$/Octavius1500 system and 2%L,3 mm PR97% (threshold 10%) for the Oct4D/Octavius1500 system. These are first line pass/check criteria and plans that fail are not necessarily rejected, but submitted to a more detailed investigation.

Conclusions: When irradiated from the front, the Octavius1500 array has two main advantages over its 729 predecessors: its instantaneous measurement stability and-–most importantly—its twofold detector density. In the Oct2D1500 phantom, these advantages are counterbalanced by the more pronounced directional dependence. The measurement-based 3D dose reconstruction in the Oct4D system, however, benefits considerably from the higher detector density in the checkerboard panel design. © *2014 American Association of Physicists in Medicine*. [http://dx.doi.org/10.1118/1.4892178]

Key words: QA, VMAT, ion chamber array, gamma evaluation

1. INTRODUCTION

Over the past decade, with the ever increasing complexity of radiotherapy treatments, two dimensional detector arrays have gained in popularity. Compared to the traditional equipment available to medical physicists such as single ion chambers or diodes, film, and water phantoms, these detector arrays present numerous advantages. They are efficient because of the simultaneous acquisition of many point doses; they are versatile, reliable, and easy to set up. Because of these characteristics, they have proven to be excellent tools for commissioning of treatment planning systems (TPS), machine QA and above all, for individual patient verification in the cases of intensity modulated (IMRT) or volumetric modulated arc therapy (VMAT). Although a lot less noisy, less error prone, a lot less time consuming, and considerably more cost-effective, they still have two key drawbacks compared to film: their detector resolution and detector density. The PTW Seven29 and Octavius729 arrays (PTW, Freiburg, Germany) (e.g., Refs. 2–6) have 729 cubic ion chambers (area 0.25 cm^2) distributed over the 27 $\times$ 27 cm^2 detector surface, resulting in 25% active area coverage. By allowing a merge of multiple measurements acquired with a shift in position in between, the detector density can be increased two- to fourfold. Although possible and certainly useful, fourfold merging is only done in special cases as it is somewhat cumbersome and quite time consuming. Furthermore, in the Verisoft 6.0 software version, this procedure is only available for planar dose measurements and not yet when measuring in the rotational Octavius® 4D (PTW, Freiburg, Germany) phantom (Oct4D).

As rotational treatments are taking up an ever increasing share of all radiotherapy treatments, the most commonly used verification methods have gradually moved from field-by-field to composite plan verification. Composite plan measurement systems produce either planar (2D)[7–13] or three dimensional (3D)[14–23] dose information. Planar data are obtained from the measurement in a straightforward manner, with data manipulation mostly limited to the application of energy (and sometimes angle) dependent calibration files and correction factors. Only the measured datapoints are subjected to gamma evaluation analysis. To obtain full 3D dosimetric information, there currently exist basically two types of 3D dosimeters: direct measurement systems (typically gels/polymers) and measurement guided 3D dose reconstruction methods from a limited data set. For the latter, the precision with which the dose can be reconstructed is inevitably dependent on the density of the acquired data points. To overcome the problem of the limited data point density, some commercially available methods reconstruct 3D dose information[7,8] by means of interpolation algorithms that exploit the dicom exported, TPS calculated dose matrix to reconstruct dose in between measurement points. Other systems have developed algorithms that do not rely on the TPS for phantom dose reconstruction.[1,11–13]

The PTW approach fundamentally opposes to the blending in of TPS information into the measurement-based dose reconstruction. The 3D dose reconstruction in the Oct4D/Octavius729 system is therefore solely based on the independently acquired depth dose curves in a water phantom and on a straightforward linear interpolation to resample the 1 cm spaced measurement grid to the final 3D dose matrix with a typical resolution of 0.25 cm in all directions.[1] The price to be paid for the TPS-independent dose reconstruction is expected to be directly related to this linear interpolation. This was confirmed by Mc Garry *et al.*[1] who validated the dosimetric and mechanical accuracy of the Oct4D/Octavius729 system and concluded it to be efficient for 3D validation of RapidArc® treatments, but who also stated that potential improvements in the device lie with closer detector spacing for better resolution. In the longitudinal direction, line profile comparisons clearly show the impact from the linear interpolation required to overcome the lack of dosimetric information in the transversal planes through the 5 mm thick detector-free lines of the 2D array. In this study, we evaluate a new PTW detector prototype, further referred to as Octavius1500, having almost the same outer dimensions and single detector size as the previous models but nearly twice the amount of ion chambers, resulting in a near 50% active area coverage.

For both comparison and validation purposes, in addition to the Octavius1500 prototype, we make use of both the original Seven29 and the currently commercially available Octavius729 ion chamber arrays in combination with their associated phantoms: the octagonal, static Oct2D^{729} phantom for planar dose measurements or the cylindrical, rotational Oct4D phantom for full 3D dose reconstruction. The original Oct2D^{729} phantom was developed for the Seven29 model. The Oct2D^{729}/Seven29 tandem was found to be a solid, reliable measurement system that can easily be used on any treatment unit, requiring no physical or electronic link to the treatment unit itself. As a drawback, it only provides dosimetric information in a single (typically horizontal) plane of measurement. To allow more complete 3D dose reconstruction, the cylindrical, rotational Oct4D phantom was developed. For use in the Oct4D phantom, the Seven29 array needed to be replaced with a detector having faster read-out capabilities, hence the release of the Octavius729 array. The latter can also handle increased dose rates (up to 48 Gy/min compared to the previous 10 Gy/min). To reduce radiation damage to the electronics of the array (most prominent when frequently used in high (20–25 MV) energy photon beams), the Octavius729 detector was also equipped with heavy shielding of the electronics and a denser base plate to obtain a mechanically robust 2D array construction. Although this dense base plate does not cause any significant problems for the Oct4D combination, it does have two disadvantages. First, whereas the Seven29 needs only very little preirradiation ($\sim$100 MU) before obtaining stable measurements, the Octavius729 detector needs considerably more warming up and suffers from relatively rapid cooling down.[1] Second, when using the Oct2D^{729} phantom in combination with this Octavius729 detector, the dense housing presents an extreme challenge to the heterogeneity correction capabilities of most dose calculation algorithms currently employed in clinical routine. We therefore continue to use the original Oct2D^{729}/Seven29 tandem. The Oct4D/Octavius729 system does not suffer from the above mentioned inconvenience as the 2D array rotates along with the gantry and is therefore always irradiated from the front.

The aim of this study is to investigate the dosimetric characteristics of the new Octavius1500 array and its associated phantoms and to compare to the previous systems.

In line with the rising amount of publications advocating the retirement of the widely used but overly lenient 3%, 3 mm (global dose) gamma analysis criteria, e.g.,[24–26] we have also focused on deriving appropriate evaluation criteria to be used with the new measurement systems in clinical routine with the Varian solution.

2. METHODS AND MATERIALS

The measurements performed in this study were carried out on two Varian 2100iX Clinacs (6 MV and 18 MV) both with a 120 Millennium MLC and both fully equipped for IMRT and RapidArc delivery. Treatment plans were optimized in the Eclipse TPS (v10.0.28) and dose calculations were performed by means of the Anisotropic Analytical Algorithm (AAA) (v10.0.28) algorithm.

The detector evaluated in this study is shown in Fig. 1(a). It is a prototype of the new Octavius1500 ion chamber array (PTW, Freiburg, Germany), consisting of 1405 vented cubic ion chambers-–of $0.44 \times 0.44 \times 0.30$ cm^3 each-–mounted below a 0.5 cm polystyrene build-up layer. The effective point of measurement is situated in the center of the detectors. The physical dimensions of the detector (housing and electronics) are $30 \times 47 \times 2.2$ cm^3. The ion chambers cover a 27×27 cm^2 active area and are arranged in a checkerboard pattern (with a center-to-center distance of 0.707 cm) instead of the uniform grid arrangement used for the 729 ion chambers in the previous 2D array models. The base plate below the ion chambers and the circuit board is made of nearly water equivalent material (polystyrene), while the electronics alongside the chambers is protected by improved shielding. The electrometer is designed to handle a dose rate of up to 48 Gy/min. As with every PTW ion chamber array, the 2D calibration matrix and the absolute calibration of the central chamber were determined in the ^{60}Co beam at the PTW secondary standard dosimetry laboratory.

This detector matrix can be used in combination with solid water plates for orthogonal measurement setups as well as with phantoms of the Octavius® series, specifically designed for multidirectional irradiation.

To assess the below phantom combinations for quality assurance of clinical treatments, first, we made use of an in-house standardized dataset containing six test patients with different treatment sites (one stereotactic lung lesion, one large lung lesion, one pelvis, one prostate and two head-and-neck). Each of these test cases contains different treatment plans, encompassing both static gantry (conformal and IMRT) and rotational (RapidArc) plans, and utilizing either the 6 MV or 18 MV photon beam. As this database is also designed for TPS commissioning and upgrade validation, all of these treatment beams (20 in total) have been subjected to extensive validation of the treatment delivery and the treatment calculation by combining all routinely established tools for treatment verification available in the department. These encompass field by field Varian portal dosimetry, field by field orthogonal verification with the Seven29 2D array in solid water (merging four shifted measurements into one to improve the effective detector density if required), field by field orthogonal verification with the PTW 1000SRS array in solid water (only for the stereotactic lung lesion), composite plan verification by means of the routinely used Oct2D^{729}/Seven29 tandem (again merging two longitudinally shifted measurements into one to improve measurement resolution if necessary) and composite plan verification by means of the Oct4D phantom in combination with the Octavius729 and 1000SRS array (the latter again only for the stereotactic lung lesion). When validating a measurement system by comparing it to TPS data, there is always the limitation of the accuracy of the TPS itself. To reduce the impact of this as much as possible, these carefully validated plans make an ideal starting point for the testing of the new 2D array and the associated octagonal phantom.

In addition to this reference set, all RapidArc routine patient treatments were added to the study until a total number of 60 plans was obtained. These included 28 prostate, ten head and neck, two rectum, one sacrum, three (stereotactic) liver, two stomach, four oesophagus, three lung, four cranial, and three metastasis treatments. All of these were also verified with the routinely established patient QA procedure based on the Varian portal dosimetry in combination with the Oct2D^{729}/Seven29 system (in horizontal position).

2.A. Octavius1500 basic dosimetric characteristics in solid water

First, the basic dosimetric characteristics of the detector were measured in a simple orthogonal setup [Fig. 1(b)]: the detector was placed below 4.3 cm of 30×30 cm^2 solid water plates (PTW, Freiburg, Germany) and on top of 5 cm of solid water to attain sufficient backscatter. In analogy to the Octavius729 characterization by McGarry *et al.*,[1] a series of measurements was performed to quantify the warm-up (and

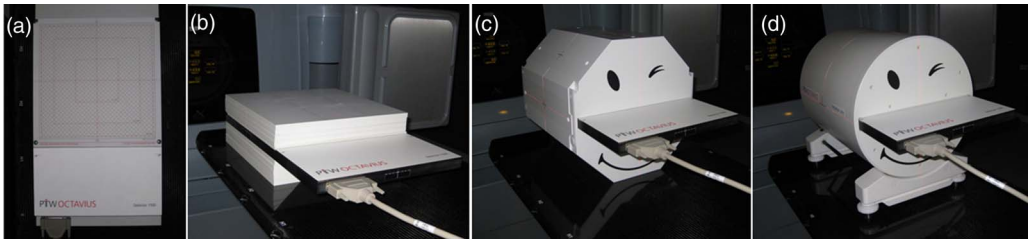

FIG. 1. (a) The Octavius1500 detector, (b) the orthogonal setup, (c) the Oct2D^{1500}/Oct1500 tandem, and (d) the Oct4D/Oct1500 tandem.

cool-down) characteristics of the new array, its dose rate dependence, its response as a function of total dose and its output factor behavior.

The detector and solid water material were always left to acclimatize long enough in the treatment room to make sure no impact from temperature changes could interfere with the results. The dose required for detector warm-up was determined by performing 20 consecutive measurements of a 10 × 10 cm^2 field with 100 MU (30 s between the start of each measurement). After the 20th measurement, the cool-down was monitored by repeating the 10 × 10 cm^2, 100 MU irradiation with ever increasing time intervals between two measurements (5, 15, and 30 min). The dose rate dependence was measured by delivering the above mentioned 10 × 10 cm^2 field (100 MU) at nominal dose rates of 100, 200, 300, 400, 500, and 600 MU/min. Similarly, the dose dependence was measured by delivering the 10 × 10 cm^2 field with 5, 10, 20, 50, 100, 500, and 1000 MU. Finally, the response of the detector as a function of field size was assessed by delivering 100 MU for square fields of 3 × 3 cm^2 to 25 × 25 cm^2. For all of the above measurements—except for the warm-up and cool-down assessment—data were averaged over three consecutive measurements. All measurements were repeated with a 0.125 cc ion chamber (T31010 Semiflex and Unidos electrometer, PTW, Freiburg, Germany) in the same solid water setup for comparison.

2.B. Octavius1500 in the octagonal Oct2D^{1500} phantom

2.B.1. Redesign of the Octavius2D phantom

The directional dependence of the original Seven29 array was reported previously and concluded to be due to the composition of the upper and lower electrodes in the array panel.[9] As the design of these electrodes has now been changed to accommodate for the higher detector density in the Octavius1500, the compensation cavity of the octagonal Oct2D phantom for use with the new Octavius1500 detector panel was also redesigned in close analogy to the development of the original Oct2D^{729} phantom:[9] The initial validation of the directional dependence was mostly done by means of static field measurements.: The Octavius1500 array was placed into the full Octavius (Oct2D^{full}), containing no compensation cavity as well as into the newly designed Oct2D^{1500}, containing a 3.9 cm compensation cavity [Fig. 1(c)]. To exclude all possible effects from the treatment couch, the phantom was rotated such that the array was in the vertical position. Data were acquired for gantry angles going from 90° to 270° (CCW) in steps of 15°. Gantry 90° and 270° correspond to orthogonal beam incidence from the front and rear of the array, respectively. For clarity, however, we will refer to these as if the array were in its horizontal position and report on gantry angles going from 0° to 180°. Data were acquired for square field sizes of 5 × 5 cm^2, 10 × 10 cm^2, and 20 × 20 cm^2 (100 MU) for 6 MV and 18 MV. Following the static field validation, a number of open field arc treatments were delivered for the above mentioned fields sizes. Irradiation through the treatment couch was again first omitted by programming a gantry rotation from 90° to 270° and by measuring with the phantom in its vertical position. Based on the entire measurement series, the dimensions of the required compensation cavity were derived to equalize the detected dose from the front and from the rear and a prototype of the new octagonal Oct2D^{1500} phantom was manufactured with a 3.9 cm wide cavity. The array was always cross-calibrated in the phantom by means of a 10 × 10 cm^2 field, delivering 296 MU for 6 MV and 254 MU for 18 MV (gantry 0° and SPD = 84 cm). For our specific Clinac calibration, this corresponds to a dose of 2 Gy at the isocenter in water equivalent conditions. This cross-calibration procedure also inherently corrects for the temperature, pressure, and energy dependence and eliminates any deviation linked to the daily machine output fluctuation. For every setup, AAA dose calculations were performed on an artificially reconstructed, water equivalent (HU = 0) homogeneous octagonal phantom in the Eclipse TPS as well as on the CT scan of the Oct2D^{full}/Oct^{1500} combination.

2.B.2. Clinical validation of the Oct2D^{1500}/Octavius1500 tandem

To assess the Oct2D^{1500}/Octavius1500 tandem [Fig. 1(c)] for quality assurance of clinical treatments, first, we made use of the in-house standardized dataset. Following this initial general validation, the 60 ensuing RapidArc patient treatments in the department were measured with the new Oct2D^{1500}/Octavius1500 tandem in addition to the routinely established patient QA procedure. For analysis in the Verisoft 6.0.1 software, the calculated 3D dose matrices as well as planar doses in the horizontal plane of measurement were exported from Eclipse. The presence of the treatment couch was taken into account during the calculations (using the default HU values provided by Varian Medical systems for the IGRT couch, i.e., −1000 HU for the couch interior and −300 HU for the shell).

All of the above treatment plans were evaluated using the range of gamma evaluation criteria listed in Table I. The reasoning behind the choice of gamma evaluation criteria is elaborated on in Sec. 2.D.

2.C. Octavius1500 in the cylindrical Oct4D phantom

The Octavius® 4D system consists of a cylindrical, rotational phantom in which the 2D array is inserted [Fig. 1(d)]. An external inclinometer mounted on the gantry provides constant feedback on the actual gantry angle and allows the control unit to rotate the phantom accordingly, keeping the 2D array perpendicular to the beam axis at all times. Thus, the orthogonal beam output can be measured from all angles and any possible directional dependence of the 2D array becomes irrelevant. The delivered dose as a function of gantry angle is stored in the measurement file. Upon loading the measurement file in the Verisoft software, for every measured gantry angle the 3D dose is reconstructed by extrapolating the data in the 2D measurement plane to the full phantom by

TABLE I. Overview of the different gamma evaluations performed on each of the phantom/array combinations: γ_{2D} denotes a gamma evaluation based on the comparison with a planar calculated dose distributions whereas γ_{3D} makes use of the full 3D calculated dose matrix. "G" stands for global dose normalization, whereas "L" denotes a local dose comparison. The different thresholds used during the evaluation are referred to as iso10%, iso50%, and iso95%. $\{\gamma\}$: 3%G/3 mm, 2%G/3 mm, 2%G/2 mm, 3%L/3 mm, 2%L/3 mm, 2%L/2 mm.

	γ_{2D} ($iso_{10\%}$)	γ_{3D} ($iso_{10\%}$)	γ_{3D} ($iso_{50\%}$)	γ_{3D} ($iso_{95\%}$)
$Oct2D^{729}$/Seven29	$\{\gamma\}$	$\{\gamma\}$		
$Oct2D^{1500}$/Octavius1500	$\{\gamma\}$	$\{\gamma\}$		
Oct4D/Octavius1500		$\{\gamma\}$	$\{\gamma\}$	$\{\gamma\}$

applying depth dose curves through every measurement point. The total 3D dose is then reconstructed as the sum of these individual contributions and interpolated linearly to a user specified dose grid. The resolution of the reconstructed 3D dose grid was set to the default values (i.e., 0.25 cm in all three directions); this is the same resolution as used during the Eclipse dose calculations. The percentage depth dose curves needed for the reconstruction were acquired in a water phantom with an ion chamber (0.125 cc Semiflex, PTW, Freiburg, Germany) for field sizes ranging from 3×3 to 27×27 cm^2. The obtained data were subsequently interpolated and converted into the format requested by the manufacturer by means of the Mephysto software (PTW, Freiburg, Germany).

Following a cross-calibration procedure near-identical to the one described for the Oct2D measurements (10×10 cm^2 field, 298 MU and 256 MU for 2 Gy cross calibration with 6 and 18 MV, respectively), all treatment plans of the reference database as well as the additional 60 RapidArc routine patient treatments were measured with the Octavius1500 inserted into the Oct4D phantom. The relative electron density of the phantom was set to be water equivalent (i.e., equal to 1.00) in the Verisoft dose reconstruction options.

The corresponding TPS dose was calculated on artificial CT data of the Octavius phantom, containing merely a cylindrical outline with diameter 32 cm. In accordance to the relative density set for the measurement reconstruction in Verisoft, the phantom was also defined to be water equivalent in Eclipse (HU = 0). The dose calculation resolution was set to 0.25 cm as this is the resolution used in clinical routine. The treatment couch was again taken into account for all calculations.

The gamma evaluations used to compare measured and calculated data are outlined in Table I and described in Sec. 2.D. The calculated dose was always loaded as the reference in dataset A, while the measurement was loaded in dataset B.

2.D. Gamma evaluation: The quest for sensible, sensitive, and efficient data analysis

To evaluate the dosimetric agreement between measured and calculated dose, we make use of the gamma evaluation method implemented in the Verisoft 6.0.1 version. This calculation of the gamma index is based on the theoretical concept of Low *et al.*,[27] including the 2nd and 3rd pass filter criteria described by Depuydt *et al.*[28] to minimize the amount of false positives in regions of steep gradients. All measurements (planar or 3D) were compared to the 3D exported dose matrix using the gamma 3D index calculation (γ_{3D}). In addition, the planar dose measurements obtained in the $Oct2D^{729}$/Seven29 and $Oct2D^{1500}$/Octavius1500 tandems were also compared to the planar dose exports. For this comparison, we have to use the 2D gamma index calculation (γ_{2D}).

As outlined in Table I, for the different phantom setups and datasets, we have performed a series of gamma evaluations for the range of criteria currently found in literature going from the most lenient 3%G,3 mm (where "G" stands for global dose normalization) to the most demanding 2%L,2 mm (where "L" stands for local dose). In addition, for the Oct4D data, we have made use of the volumetric gamma analysis tool in Verisoft, presenting statistical results on the pass rates (PR) for different isodose levels. As levels of interest, we have selected (i) the 10% isodose level, basically encompassing most of the irradiated volume, (ii) the 50% isodose, to make sure the higher dose regions (typically including organs at risk such as the spinal cord but also the low dose target volumes in simultaneous integrated boost treatments) receive the appropriate amount of attention, and (iii) the 95% isodose, as a measure for the accuracy with which the target volume coverage is reported.

To commission the use of the new 2D array and its associated phantoms, analysis was always first performed on the test patient package for which the 2%L,2 mm agreement between calculated and delivered dose had been established beforehand by combining the information from the different alternative measurement methods. Subsequently, to explore the use of the detector systems for routine pretreatment validation, the same evaluations were performed on the 60 Rapidarc patients.

3. RESULTS

3.A. Octavius1500 basic dosimetric characteristics in solid water

As can be seen from Fig. 2(a), contrary to what has been reported by McGarry *et al.*[1] on the Octavius729 2D array, the Octavius1500 shows virtually no need for preirradiation. With less than 0.2% difference between successive measurements, regardless of the time interval in between, it shows no signs of warm-up or cool-down. The dose rate dependence for dose rates typically occurring in clinical routine (e.g., between 200

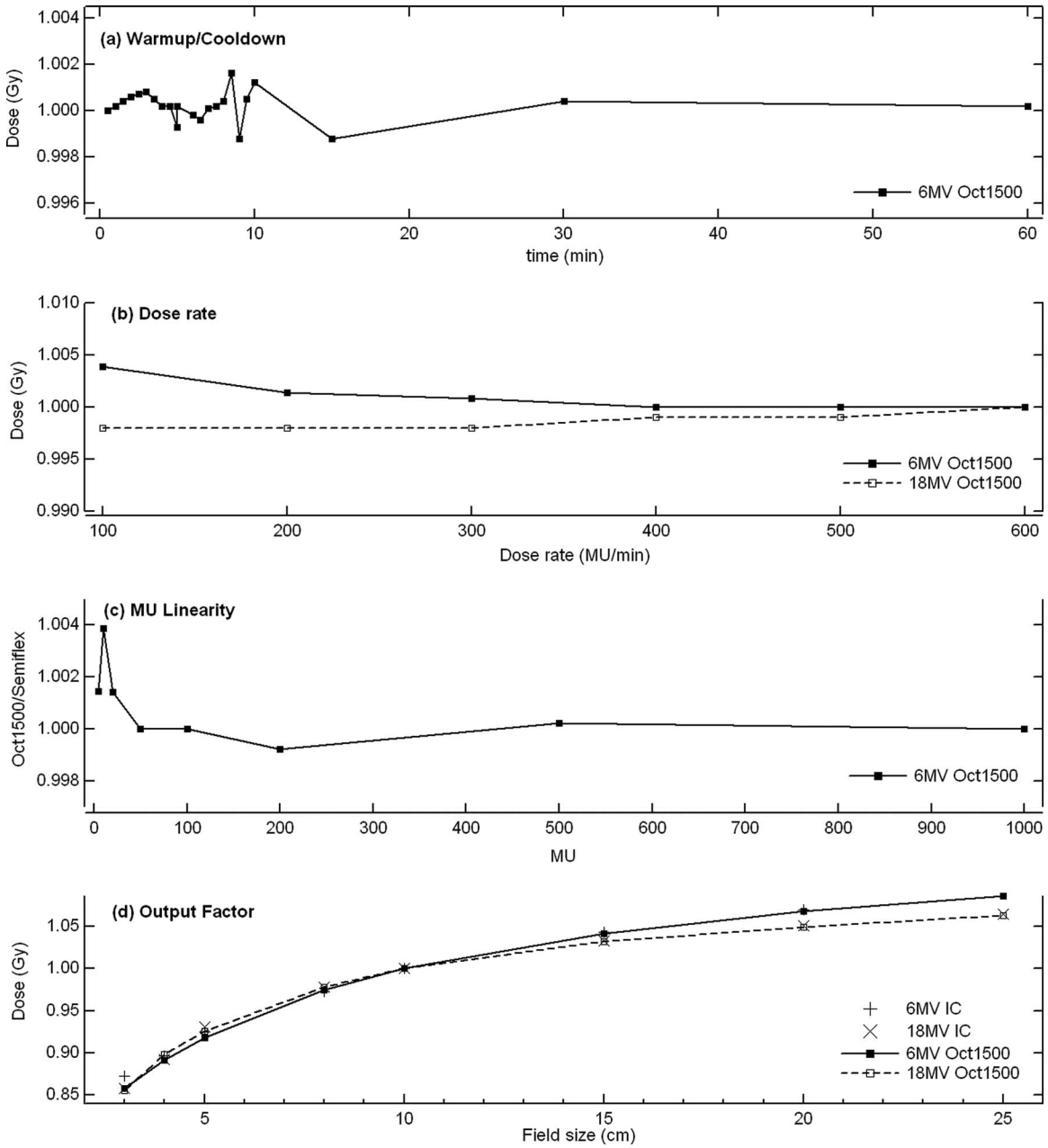

FIG. 2. Basic characteristics of the Octavius1500 2D array as measured in the rectangular solid water, showing (a) the warm-up/cool-down behavior as a function of time and successive irradiation, (b) ratio of 2D array and ion chamber (Semiflex 0.125 cc) measurements assessing the dose rate dependence for both 6 and 18 MV irradiation, (c) ratio of 2D array and ion chamber measurements assessing the detector linearity as a function of total MU, and (d) the field size dependence for 6 and 18 MV, showing the output factors measured with an ion chamber and with the 2D array.

and 1000 MU/min for flattened beams) is also beneath 0.2% and therefore within the overall reproducibility of the measurement for both energies (displayed values are the ratio between measurements performed with the 2D array and single ion chamber measurements). The absolute dose measurements as a function of MU agree with ion chamber measurements within 0.2% for 20 MU or more, and do not exceed 0.4% for even the lowest doses (5 and 10 MU). The output factors obtained with the Octavius1500 array are in agreement with the ion chamber data within 0.6% for all field sizes, except for the smallest field (3 × 3 cm) where a 1.2% deviation is observed for 6 MV.

3.B. Octavius1500 in the octagonal Oct2D^{1500} phantom

3.B.1. Redesign of the Oct2D phantom

The directional dependence of the Octavius1500 array can be observed in Fig. 3, showing the ratio between the isocentric dose calculated on the artificial homogeneous phantom (HU = 0) and the dose measured with the central chamber of the Octavius1500 2D array inserted first into the Oct2D^{full} phantom (red symbols and dashed lines) and second into the new Oct2D^{1500} phantom with the customized compensation cavity (black symbols and solid lines) The ratio between the

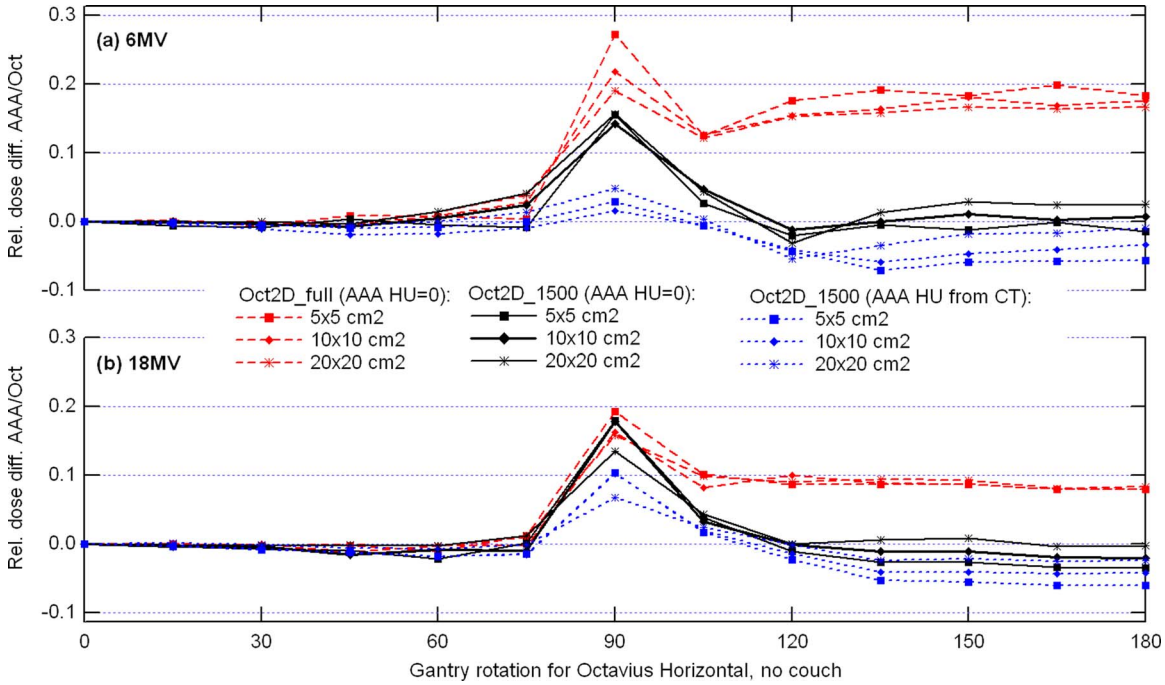

FIG. 3. Ratio between the isocentric dose calculated by AAA on the homogeneous octagonal phantom (HU = 0) and the dose measured with the central chamber of the Octavius1500 inserted first into the Oct2D^{full} phantom [(red) symbols and dashed lines] and second into the new Oct2D^{1500} phantom with the customized compensation cavity [(black) symbols and solid lines]. The ratio between the isocentric dose calculated by AAA on a CT scan of the Oct2D^{full} phantom with the Octavius1500 array *in situ* to the measured dose in the Oct2D^{1500} phantom is also displayed [(blue) symbols and dotted lines].

isocentric dose calculated by AAA on the CT scan of the Oct2D^{full} phantom with the Octavius1500 array *in situ* to the measured dose in the Oct2D^{1500} phantom is also displayed (blue symbols and dotted lines). For 6 MV, the 3.9 cm compensation cavity reduces the deviation on the beam axis for irradiation from the rear (between gantry angles 120° and 180°) from ∼ 20% to a maximum of 1.5% for the 5 × 5 and 10 × 10 fields and 2.5% for the 20 × 20 field. For the 18 MV beam, the compensation cavity slightly overcorrects the ∼10% deviation, resulting in a −2.5% maximum deviation for the 5 × 5 field and a −1.5% and 1% maximum deviation for the 10 × 10 and 20 × 20 fields, respectively. Since the compensation cavity does not extend to the side of the array, the discrepancies between calculation and measurement remains practically unaltered for lateral beam incidence. Also visible from Fig. 3, it might be worthwhile to mention that the use of a CT scan of the Oct2D^{full} phantom with the Octavius1500 array *in situ* for the AAA dose calculation does not improve the overall agreement. Reintroducing the highly complex heterogeneous structure back into the dose calculation may slightly improve the results for lateral beam incidence (mostly for 6 MV), but it considerably worsens the agreement for the rear side irradiations.

Figure 4 illustrates the results obtained for the different field sizes for the half-arcs for 6 MV and 18 MV. On the beam axis, the Oct2D^{1500} phantom design reduces the discrepancies observed with the Oct2D^{full} phantom from maximum 8.5% and 5.5% for 6 and 18 MV, respectively, to less than 1.3% for both energies and all field sizes. From Fig. 4, however, it can also be observed that the lower dose regions towards the side of the 2D array around which the half arc was rotated (i.e., the left side of the dose profiles on the graph), are less well reproduced by the measurement. These lower dose regions coincide with the portion of the 2D array for which the relative contribution of the uncompensated lateral dose is the largest: for anterior and posterior irradiation directions, this area is shielded by the collimator jaws, whereas for lateral irradiation, this is precisely the area situated in the upper part of the photon depth dose curve.

3.B.2. Validation of the Oct2D^{1500}/Octavius1500 tandem

An overview of the scores (mean and standard deviation) obtained for the horizontal plane of measurement with the different gamma evaluation criteria for the reference and routine patient dataset is given in Table II.

As the reference dataset has been validated with multiple measurement methods that—combined—result in the conclusion that the actual agreement between delivery and calculation is meeting the 97% PR for 2%L,2 mm for all plans included, the observed scores are a good indication of the additional measurement uncertainties that should be attributed to the Oct2D measurement systems.

For the reference plans, the original Oct2D^{729}/Seven29 combination achieves a near 100% PR for all global gamma evaluations. The local gamma evaluations score less—as expected—but only slightly and only for the strictest dose difference criteria (2%L): the most demanding 97% PR, 2%L,2 mm criteria are still met for 15 out of 20 plans when using the 3D dose for comparison rather than the planar dose export (13 out of 20 pass). Increasing the DTA to 3 mm suffices

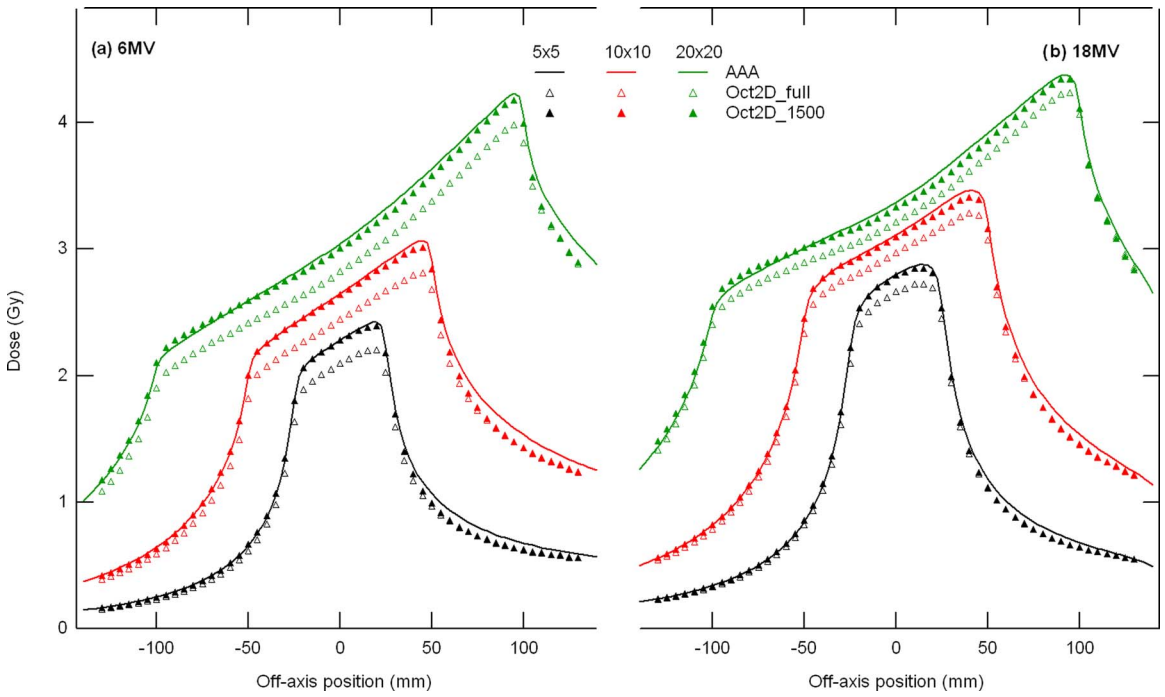

FIG. 4. Calculated and measured dose profiles for half arc open field treatments with different field sizes: 5 × 5 cm^2, 10 × 10 cm^2, and 20 × 20 cm^2. The dose was calculated with AAA (solid lines) in the artificially created, water equivalent homogeneous phantom. The measurements were performed with the Octavius1500 2D array inserted into the Oct2D^{full} (open symbols) and Oct2D^{1500} (solid symbols) phantom.

to obtain the 97% PR for all plans for the 3D gamma and for 18 out of 20 plans for the 2D gamma calculation. Gamma evaluations for the new Oct2D^{1500}/Octavius1500 combination score consistently less and show a larger standard deviation, indicating a wider spread of the scores around the displayed mean value. The 97% PR is only reached for all reference plans when applying the 3%G,3 mm criteria (for both 2D and 3D gamma calculations). Tightening the global dose difference limit to 2% considerably reduces the mean score and increases the standard deviation. Albeit expected, the decrease in score when switching from global to local dose criteria is also more pronounced for the new Octavius system. Upon inspection of the individual data, it can be seen that most of the observed deviations relate back to the uncorrected lateral dose incidence. Pass rates for static gantry deliveries (IMRT and conventional) are very dependent on whether or not the treatment includes lateral beam incidence and on the relative dose contribution of the latter. For arc treatments, while the dose measured within the target volume is in good agreement with the calculated dose, a very important fraction of the points that fail are to be found in the lower dose area, i.e., outside of the target dose area. In agreement with the deviations observed in these areas for the half-arc open field data displayed in Fig. 4, Fig. 5 illustrates the same issue appearing in the dynamic treatment plans: the blue and red squares indicate measurement points that do not meet the gamma criteria. Whereas the failed points within the PTV area are dispersed and indicate both too low (blue squares) or too high (red squares) dose, outside of the target area the general tendency is clearly that the measured dose is lower than the calculated dose. Going from 2%G to 2%L dose shows that the increase in failed points is situated almost entirely in this area and with the threshold set to 10% of the maximum (calculated) dose, nearly all of these out-of-field measurement points contribute to the new gamma score. The transversal line profile confirms

TABLE II. Results of the Oct2D^{1500}/Octavius1500 gamma analysis: Mean and standard deviation values of the gamma evaluation scores obtained for the horizontal plane of measurement with the different gamma criteria indicated in the table. All analysis was performed with a dose threshold set to 10% of the maximum dose. The gamma index was calculated for both the planar (γ_{2D}) and volumetric (γ_{3D}) dose export. The upper half shows the results on the reference dataset whereas the results of the routine RapidArc patient dataset are given in the lower half of the table. For comparison, results obtained with the routinely used Oct2D^{729}/Seven29 tandem are also given for both datasets.

	Oct2D^{1500}/Octavius1500		Oct2D^{729}/Seven29	
	$\gamma_{3D}(iso_{10\%})$	$\gamma_{2D}(iso_{10\%})$	$\gamma_{3D}(iso_{10\%})$	$\gamma_{2D}(iso_{10\%})$
Reference dataset				
3%G,3 mm	99.40 ± 1.13	98.93 ± 1.33	100.00 ± 0.00	100.00 ± 0.00
2%G,3 mm	97.31 ± 3.56	95.93 ± 4.57	100.00 ± 0.00	99.99 ± 0.04
2%G,2 mm	95.77 ± 4.60	93.83 ± 5.78	99.99 ± 0.06	99.95 ± 0.13
3%L,3 mm	97.60 ± 3.61	95.26 ± 5.48	99.82 ± 0.53	99.67 ± 0.65
2%L,3 mm	95.55 ± 4.82	92.41 ± 6.78	99.74 ± 0.73	98.69 ± 2.18
2%L,2 mm	92.44 ± 9.28	88.25 ± 8.27	97.85 ± 2.53	97.23 ± 3.44
60 RA patients				
3%G,3 mm	98.82 ± 1.15	97.82 ± 1.85	99.95 ± 0.16	99.97 ± 0.09
2%G,3 mm	97.47 ± 2.21	95.21 ± 3.26	99.89 ± 0.35	99.62 ± 0.72
2%G,2 mm	93.78 ± 3.59	90.91 ± 4.70	99.77 ± 0.38	99.24 ± 1.39
3%L,3 mm	97.14 ± 2.16	93.87 ± 3.77	99.36 ± 1.38	99.46 ± 0.71
2%L,3 mm	96.55 ± 2.69	92.51 ± 4.17	99.66 ± 0.41	99.01 ± 0.79
2%L,2 mm	91.19 ± 4.45	85.82 ± 5.92	97.97 ± 1.71	97.72 ± 1.80

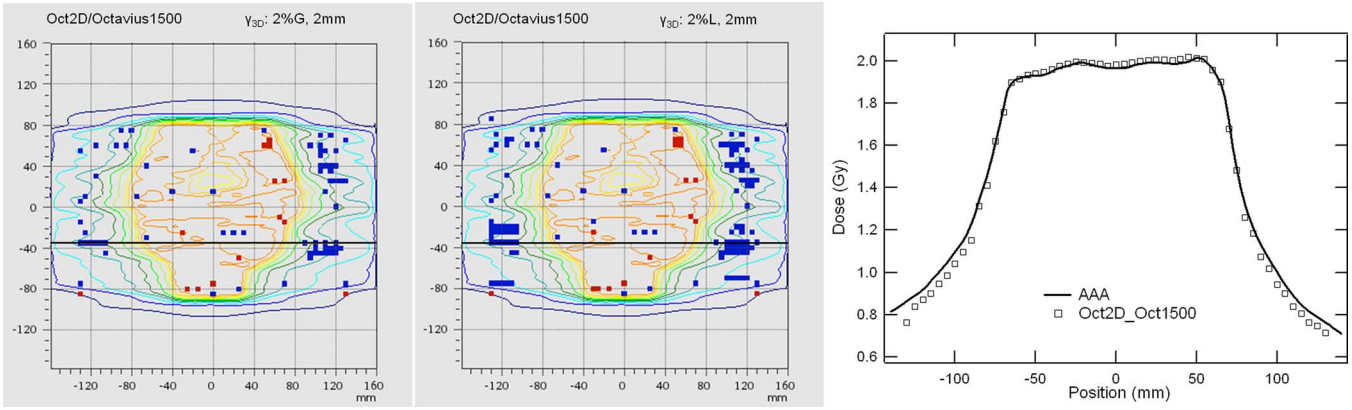

FIG. 5. Gamma evaluations illustrating the increase in failed points outside of the target dose area when switching from 2%G,2 mm to 2%L,2 mm. The line profile reveals the too low dose measurement in these areas. The solid horizontal line on the gamma maps indicates the position of this transversal line profile. Within the target dose area, failed points are scattered, both cold and hot and almost identical between both gamma evaluation modes. The displayed example is a pelvic RapidArc plan.

the observation. Cross-validation with the Oct2D[729]/Seven29 system (not shown) confirms that this is a characteristic of the new Oct2D[1500]/Octavius1500 tandem rather than a true deviation between calculation and delivery.

The results obtained from the 60 RapidArc patients treated in routine are listed in the bottom part of Table II and show a tendency that is very similar to the one observed for the reference dataset, albeit with a smaller spread around the mean pass rate. The reduced spread is due to the fact that the reference dataset also contains static gantry treatments which show either considerably better or considerably worse pass rates, depending on whether or not the treatment includes lateral gantry angles. As expected, volumetric gamma evaluations are consistently better than planar gamma calculations, although this effect is again more pronounced for the Octavius1500 than for the Octavius729 system. The 2%L,3 mm evaluation criteria that can be used for the Octavius729 tandem need to be increased to 3%L,3 mm in order to meet the 97% pass rate for the majority of the tested patients when applying the 10% dose threshold. Within the high dose areas, results for the two Octavius tandems are comparable and the most prominent difference between the gamma maps of both systems is again clearly situated in the lower out-of-target dose regions.

3.C. Octavius1500 in the cylindrical Oct4D phantom

Table III provides an overview of the results obtained from the comparison between the Octavius1500 dose measurements in the Oct4D phantom and the corresponding 3D dose calculation exported from the treatment planning system. The table lists the mean gamma scores (and the corresponding standard deviations) obtained with the volumetric analysis tool for the six sets of gamma criteria and the three different dose thresholds.

The upper part of the table lists the results obtained on the reference dataset containing static as well as dynamic treatments for both energies. When applying the 10% dose level threshold to this dataset, the mean score exceeds 99% for all but the strictest (2%L, 2 mm) evaluation criteria and the small standard deviation reflects the very narrow spread of the individual scores around this high mean value. While reducing the DTA from 3 mm to 2 mm does lower the scores, the 97% PR is still met for most of the plans (16 out of 20). When analyzing the scores obtained with a DTA of 3 mm, we observe no significant change when restricting the dose difference from the most tolerant 3%G down to the most stringent 2%L level. As all data points with dose values down to the 10% isodose level are included in the analysis, this implies that the measured dose reconstruction is of good local accuracy down to the 10% dose level. When zooming in on the 50% and 95% isodose volumetric analysis, no significant change in the average score is observed when local rather than global dose

TABLE III. Results of the Oct4D/Octavius[1500] gamma analysis: Mean and standard deviation values of the volumetric gamma evaluation scores obtained for the different gamma criteria indicated in the table. Analysis was performed with a dose threshold set to 10%, 50%, and 95% of the maximum dose. The upper half shows the results on the reference dataset whereas the results on the routine RapidArc patient dataset are given in the lower half of the table.

	Oct4D/Octavius1500		
	$\gamma_{3D}(\text{iso}_{10\%})$	$\gamma_{3D}(\text{iso}_{50\%})$	$\gamma_{3D}(\text{iso}_{95\%})$
Reference dataset			
3%G,3 mm	99.99 ± 0.02	99.99 ± 0.04	99.92 ± 0.18
2%G,3 mm	99.92 ± 0.10	99.87 ± 0.15	99.38 ± 1.13
2%G,2 mm	99.31 ± 0.37	99.15 ± 0.48	97.84 ± 2.50
3%L,3 mm	99.99 ± 0.02	99.99 ± 0.02	99.92 ± 0.18
2%L,3 mm	99.72 ± 0.44	99.76 ± 0.31	99.31 ± 1.27
2%L,2 mm	97.98 ± 1.26	98.48 ± 0.87	97.65 ± 2.71
60 RA patients			
3%G,3 mm	99.95 ± 0.11	99.92 ± 0.28	99.47 ± 1.95
2%G,3 mm	99.77 ± 0.25	99.65 ± 0.58	97.62 ± 4.58
2%G,2 mm	98.88 ± 0.74	98.59 ± 1.09	94.60 ± 6.67
3%L,3 mm	99.89 ± 0.21	99.92 ± 0.28	99.47 ± 1.95
2%L,3 mm	99.69 ± 0.32	99.64 ± 0.59	97.57 ± 4.62
2%L,2 mm	97.40 ± 1.30	98.09 ± 1.44	94.03 ± 7.07

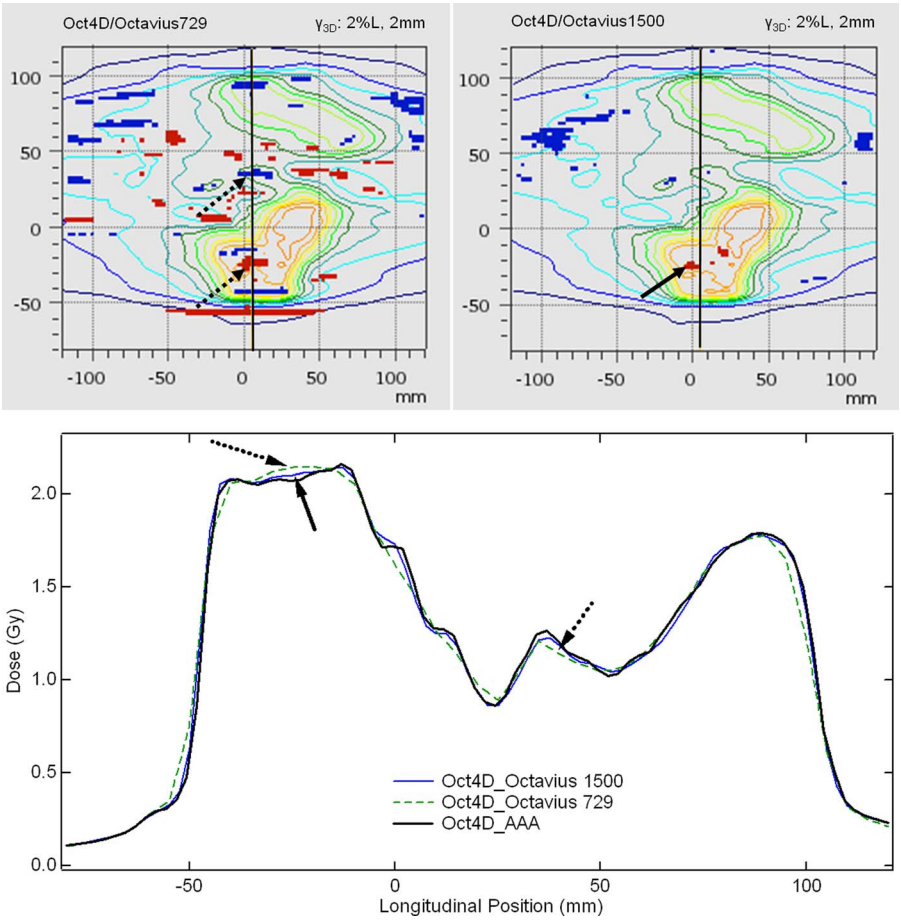

FIG. 6. Gamma evaluations (2%L,2 mm) and line profile illustrating the impact of the twofold detector density on the volumetric dose reconstruction when comparing the Oct4D/Octavius729 to the Oct4D/Octavius1500 system. The solid vertical line on the gamma maps indicates the position of the displayed longitudinal line profile. The positions indicated by the arrows on the line profile correspond to the positions indicated in the gamma map and point out some typical examples of the observed discrepancies related to the data interpolation.

criteria are applied. This again implies that with the current 3D dose reconstruction algorithm, all dose levels are covered with good precision.

The results of the volumetric gamma analysis on the RapidArc patient database shown in the lower half of Table III are consistent with the reference database, albeit with slightly smaller average scores and a slightly wider spread. The decrease in score and increase in spread is most prominent for the analysis of the 95% isodose volume, within which most of the treatment plans now fail the 97% pass rate for the strictest 2% (L or G), 2 mm gamma criteria. Upon closer inspection of the individual plans, two observations could be made. First, it was found that performing an automatic alignment between the measured and calculated dose improved some of the results. The shift proposed by the Verisoft software varied between the different plans but never exceeded ±1.5 mm in either direction. In contrast to the reference dataset which was acquired in one single measurement session with a meticulously verified phantom setup, the patient database was acquired gradually over different routine patient QA sessions, resulting in possible variations of the order of 1 mm in the phantom setup. Second, from the visual inspection of line profiles through the failed points, it can be seen that the interpolation procedure necessary to reconstruct the 3D dose from the planar measurements can give rise to the occasional failed gamma point, although the fraction of failed points is considerably less than what was previously observed on the Oct4D/Octavius729 system. The beneficial impact of the improved detector density on the gamma scores was suggested by McGarry *et al.* and is clearly confirmed through the results obtained with the patient database. Figure 6 presents a typical example, showing the 2%L,2 mm gamma analysis in the sagittal plane for Oct4D measurements obtained with the Octavius729 as well as with the Octavius1500 detector panel. The black line on the gamma analysis map indicates the position of the displayed line profile. The positions indicated by the arrows on the line profile correspond to the positions indicated in the gamma map. They point out some typical examples of the observed discrepancies related to the data interpolation. In this longitudinal profile, the improved reproduction of, e.g., the "steps" and the field edge is clearly visible.

4. DISCUSSION

While the new Octavius1500 2D array shows equally good basic dosimetric properties as the previous 2D array models

(Seven29 and Octavius729), it presents some additional advantages. First and most importantly, it has twice the detector density and because of the checkerboard design, it has no lines without detectors. Compared to the original Seven29, it has better shielding of the electronics, can handle higher dose rates, and has faster read-out times (100 ms). Compared to the Octavius729, it shows excellent reproducibility and measurement stability regardless of whether it has been preirradiated or left unused for more than a few minutes. This is especially an advantage during routine patient QA, when preirradiation (or even intermediate reirradiation to prevent cooldown) takes up valuable Linac and physicist time.

The transition from the previous 2D array models to the Octavius1500 is straightforward for field by field verification with solid water plates and for three dimensional dose measurements in the Oct4D phantom. None of these require a change in phantom or a change in procedure and the benefits from the near 50% active area coverage and the instantaneous measurement stability are irrefutable.

However, as the directional dependence of the new array differs from that of the previous models, the Octavius1500 requires a different compensation cavity when used in the octagonal Oct2D phantom. The Oct2D^{729}/Seven29 system was developed using calculations performed on a CT scan of the full phantom with the 2D array *in situ*.[9] This provided better modeling of the lateral beam incidences as the Seven29 consists of alternating bands containing either 27 or no chamber cavities at all. The 5 mm wide solid bands containing no chamber cavities have a visible impact on the shape of the longitudinal field profiles for lateral beam incidence. The improved agreement when using a CT scan with the array in place versus a totally homogeneous phantom scan was confirmed by Hussein *et al.*[26] The use of the scanned 2D array for dose calculations, however, does present some disadvantages. First, it requires a dose calculation algorithm with advanced heterogeneity correction. Second, especially for the lower energies (e.g., 6 MV), the presence of the individual chambers gives rise to ripples in the open field dose profiles, complicating the analysis as well as the choice of the reference dose level in the cross-calibration procedure.[26] Third, if an additional measurement is performed with the array in the vertical position, this also requires an additional dose calculation (and export) on a separate CT scan with the array in the corresponding vertical position. Because of its checkerboard layout, the Octavius1500 array no longer has these uninterrupted dense bands containing no ion chamber cavities. The relative profile shape of an open field irradiating the array from the side is very close to the relative profile shape that would be measured in water. Therefore, the new Oct2D^{1500}/Octavius1500 system was developed to be used with dose calculations performed on a full, homogeneous octagonal phantom, rather than on a scan with the 2D array *in situ* and the above mentioned disadvantages are no longer applicable. Because of the pronounced directional dependence, a compensation cavity of 39 mm was chosen to obtain the best compromise for all field sizes and both tested energy modes. As with the previous Oct2D^{729}/Seven29 system, the compensation cavity does not extend to the sides of the 2D array (as this would require a too large phantom), leaving the absolute deviation of the lateral dose incidence unaccounted for. Whereas this left a 2%–3% deviation between calculated and measured lateral dose in the previous system,[9,26] it leaves a 15%–20% lateral deviation in the current system (and calculating the dose on the CT scan of the phantom with the Octavius1500 *in situ* no longer offers a solution). The dosimetric impact of this can be substantial for composite plan analysis of static gantry (IMRT) plans that contain lateral fields. For RapidArc treatments, the contribution of the lateral irradiation is only a fraction of the total dose in the target and its impact is mostly seen in the lower, out-of-target dose areas towards the side of the 2D array. This is the main reason why the gamma scores in the Oct2D^{1500}/Oct1500 system are inferior to what is obtained with the Oct2D^{729}/Seven29 system. In the current Verisoft version, the impact can not be removed from the final gamma score as the dose threshold is limited to 30% of the maximum dose. Although this does affect the gamma evaluation score, in most cases, the effect is easily diagnosed in the planar display of the gamma analysis.

For the Oct4D/Octavius1500 combination, the 3D dose reconstruction unmistakably benefits from the improved resolution. Additionally, the introduction of the pass-filter criteria in the gamma evaluation of the Verisoft 6.0 software version is also expected to have a beneficial impact on the obtained pass rates. The pass rates reported by McGarry *et al.*[1] on the Oct4D/Octavius729 system of 99.2% $\pm$ 0.8% for 3%G,3 mm and 94.0% $\pm$ 3.5% for 2%G,2 mm (10% dose threshold) are now up to nearly 100% (99.99% $\pm$ 0.02% and 99.31 $\pm$ 0.37, respectively) for both sets of criteria. The sole impact of the new software version on these increased pass rates was quantified through a personal communication with McGarry *et al.*: by re-evaluating 171 patient data with the Verisoft 6.0 software version, they found a noticeable rise in the 2%,2 mm average pass rate from 93.6% $\pm$ 3.1% to 95.6% $\pm$ 1.8%. The additional improvement in the pass rates observed with the Oct4D/OCtavius1500 system can therefore be ascribed to the improved array resolution. A mean pass rate exceeding 97% is obtained for even the most stringent 2%L,2 mm gamma criteria with a 10% dose threshold. Although the interpolation between measurement points can still give rise to some failed points, these are now mostly restricted to the high dose areas (95% dose threshold) which are formed by highly modulated contributions from different gantry angles. The different planar views (sagittal, transversal, and coronal) help provide an overview and facilitate the selection of possible areas of interest to be subjected to further visual inspection. We have found the 10% and 50% dose thresholds useful to assure correct overall dose delivery in the organs at risk as well as in the lower target dose regions. The 95% dose level provides useful insights in the dose coverage of the (high dose) target.

Having tested the new Octavius1500 measurement systems, it would be all too easy to conclude that they are both of sufficient precision to largely meet the AAPM TG-119 (Ref. 29) recommended passing rate action levels of 88% (or even the somewhat more demanding and more clinically used passing rate level of 95%) with 3%G,3 mm gamma criteria. This is especially so for the Oct4D/Octavius1500 system for

which the lowest score obtained with these criteria within the whole database was 97.8%. We would, however, prefer to join Nelms *et al.*[24] in making a case for the revision of the way in which the gamma analysis is used in clinical practice. Rather than suggesting sufficiently large, universal acceptance criteria to ensure the continued use of the relatively insensitive, binary approach of the gamma evaluation (either pass or fail), we would advocate the use of more selective, equipment specific gamma criteria, all starting from the same, very strict acceptance criteria but adding measurement uncertainty to these. The primary goal of the treatment QA should be to intercept discrepancies that would result in a clinically relevant difference between the calculated and "real" dose distributions. Because during pretreatment QA, the "real" dose is represented by its measurement, first, it is the responsibility of the medical physicist to understand the limitations or inaccuracies of his or her specific measurement system and its analysis software. This should allow the physicist to decide whether or not an observed deviation is real or simply measurement related. Second, even for deviations that are judged to be real, no universal criteria can be defined regarding their clinical relevance as these are largely dependent on the location, on the treatment site and on the presence of organs at risk. So, rather than using the gamma analysis as a universal pass/fail filter, we would prefer to exploit it as a pass/check filter, only letting plans pass the first line automatic validation when we can be confident that no clinically relevant deviations are to be expected.

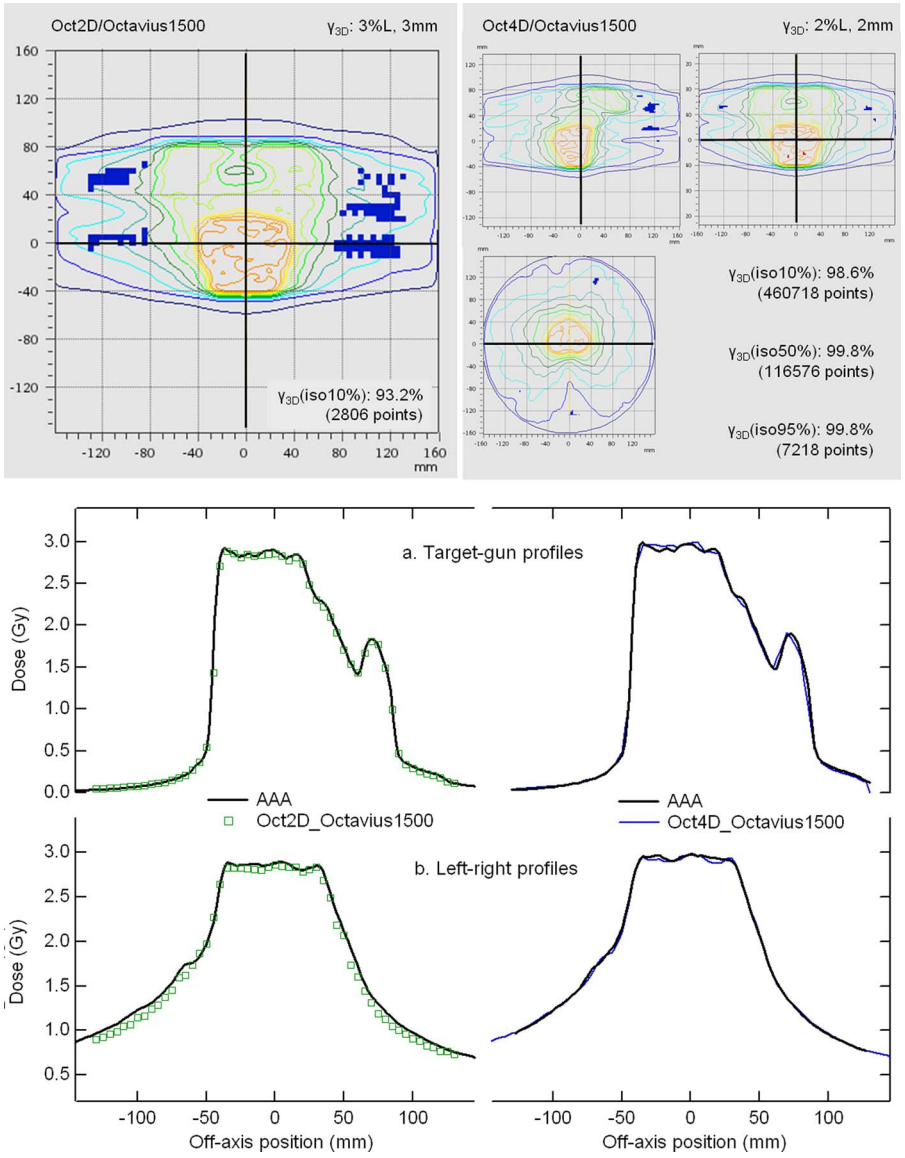

FIG. 7. Comparative example of routine treatment QA performed with the planar Oct2D[1500]/Oct1500 (left) and volumetric Oct4D/Octavius1500 (right) system. For the Oct2D[1500] system, the measurement fails to pass the γ_{3D} 3%L,3 mm PR97% (10% threshold) and is subjected to further visual inspection: The pattern of the out-of-target dose deviations is easily recognizable as a blue out-of-target shadow towards the side of the detector panel and the transversal line profiles quickly provide a visual confirmation that the deviation is of the expected magnitude. The right-hand side of the figure shows the data acquired with the Oct4D/Octavius1500 system on the same treatment plan. Although this plan passes the pass/check filter [γ_{3D} 2%L,3 mm 97%PR (10% threshold)], it serves to demonstrate the additional visual and numerical analysis tools used when data need to be subjected to a more rigourous inspection [statistical volumetric gamma analysis for different isodose levels (10%, 50%, and 95%) and visual inspection of the gamma maps in different planes and line profiles through failed points.]

For now, as an initial starting point, we will assume that no clinically relevant changes are expected when the delivered ("real") and calculated doses in the homogeneous phantom agree within 2%L, 2 mm for almost the entire irradiated volume (e.g., for 97% of the volume receiving at least 10% of the maximum dose). These starting criteria should be subjected to regular re-evaluation as radiotherapy systems further improve, but with a state of the art, properly commissioned, high quality radiotherapy system (comprised of a dose calculation and dose delivery system), this overall agreement between the calculated and the actual dose should be achievable in a homogeneous phantom for all but the lowest doses. Since such an agreement between delivered and calculated dose has been established beforehand for all plans in the reference dataset, the measurements acquired for this dataset with the Octavius1500 systems allow us to deduce the inherent limitations of the new systems. First, the small but significant drop in the gamma score when going from 2%L,3 mm to the 2%L,2 mm criteria was noticed in all Octavius tandem systems and indicates that a DTA of 2 mm might be too demanding in routine patient QA. Automatic realignment of the acquired data confirms that the precision with which the phantom and array are set up during routine QA is in the order of 1 mm. Furthermore, for the Oct2D^{1500}/Octavius1500 tandem, we know from the open arc measurements that an additional 1.5% absolute dose imprecision needs to be taken into account if we want to cover all field sizes and energies with the same criterion. Also, we are likely to encounter deviations in the out-of-target dose area because of measurement artifacts from lateral beam incidence. To account for the first known uncertainty, we have relaxed the dose criterion to 3%L. However, regarding the out-of-target dose, rather than relaxing the dose criteria further (by, e.g., moving to global dose analysis or increasing the threshold to a rather high level) and hereby risking missing important deviations in the other areas as well, we prefer to simply leave it at that and visually inspect those plans that fail the final 3%L, 3 mm 97% PR (10% threshold). Although this may imply that a substantial fraction of the plans will indeed have to be inspected, it needs to be said that for the planar dose measurements, such a gamma map inspection in the Verisoft software is very straightforward and simultaneously available on screen, together with the statistical gamma evaluation results.

An example of such an analysis is displayed in Fig. 7. The pattern of the out-of-target dose deviations is easily recognizable as a blue out-of-target shadow towards the side of the detector panel and line profiles quickly provide a visual assessment whether the deviation is of the expected magnitude. As the Oct4D/Octavius1500 system does not suffer from these absolute dosimetric imprecisions, the 1 mm concession on the DTA is the only measurement uncertainty we include in the initial pass/check step for the rotational phantom. The right side of Fig. 7 shows some of the analysis tools used for the Oct4D/Octavius1500 data acquired on the same treatment plan for which the Oct2D^{1500} plan analysis is shown on the left side of the figure. Plans that do not pass the 2%L,3 mm 97%PR (10% threshold) analysis are subjected to a more rigorous inspection, e.g., by means of the statistical volumetric gamma analysis for different isodose levels (95% and 50%) and by visual inspection of the 3D dose comparison to evaluate whether or not the dose deviation is situated in a critical area. For example, a 4% underestimated dose in a low dose area could be real but would only be of importance if a critical organ was situated in this low dose area. Even then, it would need to be looked into whether the calculated dose volume histogram on this critical organ still allows for some dosimetric margin or not. In case of doubt, reconstruction of the patient's DVH starting from the measured dose could provide help in quantifying the clinical impact of possible deviations. Such patient dose reconstruction algorithms and software tools are being developed and are also introduced in the Verisoft software. When based on reliable measurements with sufficient precision and powerful patient dose reconstruction algorithms, they could indeed provide the feedback needed to selectively judge deviations, but their evaluation and the discussion of possible limitations are beyond the scope of this study and will be part of future work.

5. CONCLUSION

With its twofold detector density, its high dose rate capability and its immediate measurement stability, the Octavius1500 outperforms its predecessors from the PTW 729 2D ion chamber array series.

For the octagonal Oct2D^{1500}/Octavius1500 system, compared to the Seven29 array tandem, the advantages of the improved resolution of the Octavius1500 system are counterbalanced by the more pronounced lateral dose deviations. Taking the observed measurement uncertainties of this Octavius tandem into account, we use 3%L,3 mm 97%PR (threshold 10%) gamma criteria to provide us with a first line pass/check filter for the routine analysis of patient treatment plans. Plans that do not pass the initial validation are not necessarily rejected but undergo additional visual analysis of the gamma distribution map and associated line profiles to assess the clinical relevance of the observed deviations.

When used in the cylindrical Oct4D/Octavius1500 system, the impact from the new checkerboard ion chamber design is even more pronounced as it results in an improved 3D dose reconstruction compared to the previous Octavius729 2D array system. With the directional dependence out of the equation and the 3D dose reconstruction improved, the gamma criteria for the pass/check inquiry could be reduced to 2%L, 3 mm 97% PR over the whole irradiated volume (threshold 10%). Only data that fail these stringent pass criteria are subjected to further investigation.

ACKNOWLEDGMENTS

The authors would like to thank PTW (Freiburg, Germany) for their enthusiasm, their support, and for providing the dosimetric equipment.

[a]Author to whom correspondence should be addressed. Electronic mail: ann.vanesch@7sigma.be

[1]C. K. McGarry, B. F. O'Connell, M. W. D. Grattan, C. E. Agnew, D. M. Irvine, and A. R. Hounsell, "Octavius 4D characterization for

flattened and flattening filter free rotational deliveries," Med. Phys. **40**, 091707 (11pp.) (2013).
[2]B. Poppe, A. Blechschmidt, A. Djouguela, R. Kollhoff, A. Rubach, K. C. Willborn, and D. Harder, "Two-dimensional ionization chamber arrays for IMRT plan verification," Med. Phys. **33**(4), 1005–1015 (2006).
[3]M. Bakhtiari, L. Kumaraswamy, D. W. Bailey, S. de Boer, H. K. Malhotra, and M. B. Podgorsak, "Using an EPID for patient-specific VMAT quality assurance," Med. Phys. **38**(3), 1366–1373 (2011).
[4]E. Spezi, A. L. Angelini, F. Romani, and A. Ferri, "Characterization of a 2D ion chamber array for the verification of radiotherapy treatments," Phys. Med. Biol. **50**(14), 3361–3373 (2005).
[5]B. Poppe, T. S. Stelljes, H. K. Looe, N. Chofor, D. Harder, and K. Willborn, "Performance parameters of a liquid filled ionization chamber array," Med. Phys. **40**, 082106 (14pp.) (2013).
[6]B. Poppe, A. Djouguela, A. Blechschmidt, K. Willborn, A. Ruhmann, and D. Harder, "Spatial resolution of the 2D ionization chamber arrays fro IMRT dose verification: Single detector size and sampling step width," Phys. Med. Biol. **52**, 2921–2935 (2007).
[7]S. Korreman, J. Medin, and F. Kjær-Kristoffersen, "Dosimetric verification of RapidArc treatment delivery," Acta Oncol. **48**, 185–191 (2009).
[8]J. L. Bedford, Y. K. Lee, P. Wai, C. P. South, and A. P. Warrington, "Evaluation of the Delta4 phantom for IMRT and VMAT verification," Phys. Med. Biol. **54**, N167–N176 (2009).
[9]A. Van Esch, C. Clermont, M. Devillers, M. Iori, and D. P. Huyskens, "On-line quality assurance of rotational radiotherapy treatment delivery by means of a 2D ion chamber array and the Octavius phantom," Med. Phys. **34**(10), 3825–3837 (2007).
[10]V. Chandraraj, S. Stathakis, R. Manickam, C. Esquivel, S. S. Supe, and N. Papanikolaou, "Comparison of four commercial devices for RapidArc and sliding window IMRT QA," J. Appl. Clin. Med. Phys. **12**(2), 338–349 (2011).
[11]V. Feygelman, G. Zhang, C. Stevens, and B. E. Nelms, "Evaluation of a new VMAT QA device, or the "X" and "O" array geometries," J. Appl. Clin. Med. Phys. **12**(2), 3346 (2011).
[12]L. Masi, F. Casamassima, R. Doro, and P. Francescon, "Quality assurance of volumetric modulated arc therapy: Evaluation and comparison of different dosimetric systems," Med. Phys. **38**, 612–621 (2011).
[13]F. Garcia-Vincente *et al.*, "Sensitivity of a helical diode array device to delivery errors in IMRT treatment and establishment of tolerance levels for pretreatment QA," J. Appl. Clin. Med. Phys. **13**(1), 111–123 (2012).
[14]H. Zhen, B. E. Nelms, W. A. Tomeé, and W. A. Tome, "Moving from gamma passing rates to patient DVH-based QA metrics in pretreatment dose QA," Med. Phys. **38**(10), 5477–5489 (2011).
[15]P. Carrasco, N. N. Jornet, A. Latorre, T. Eudaldo, A. A. Ruiz, and M. Ribas, "3D DVH-based metric analysis versus per-beam planar analysis in IMRT pretreatment verification," Med. Phys. **39**(8), 5040–5049 (2012).
[16]M. Stasi, S. Bresciani, A. Miranti, A. Maggio, V. Sapino, and P. Gabriele, "Pretreatment patient-specific IMRT quality assurance: A correlation study between gamma index and patient clinical dose volume histogram," Med. Phys. **39**(12), 7626–7634 (2012).
[17]A. J. Olch, "Evaluation of the accuracy of 3DVH software estimates of dose to virtual ion chamber and film in composite IMRT QA," Med. Phys. **39**(1), 81–86 (2012).
[18]B. E. Nelms *et al.*, "VMAT QA: Measurement-guided 4D dose reconstruction on a patient," Med. Phys. **39**(7), 4228–4238 (2012).
[19]V. Feygelman *et al.*, "Motion as a perturbation: Measurement-guided dose estimates to moving patient voxels during modulated arc deliveries," Med. Phys. **40**(2), 021708 (1pp.) (2013).
[20]D. Opp, B. E. Nelms, G. Zhang, C. Stevens, and V. Feygelman, "Validation of measurement-guided 3D VMAT dose reconstruction on a heterogeneous anthropomorphic phantom," J. Appl. Clin. Med. Phys. **14**(4), 70–84 (2013).
[21]J. Godart, E. Korevaar, R. Visser, D. Wauben, A. van´t Veld, "Reconstruction of high-resolution 3D dose matrix measurements: error detection capability of the COMPASS correction kernel method," Phys. Med. Biol. **56**, 5029–5043 (2011).
[22]R. Boggula, F. Lorenz, L. Müller, M. Birkner, H. Wertz, F. Stieler, V. Steil, F. Lohr, and F. Wenz, "Experimental validation of a commercial 3D dose verification system for intensity-modulated arc therapies," Phys. Med. Biol. **55**, 5619–5633 (2010).
[23]B. MC McCurdy, L. Mueller, E. Backman, S. Venkataraman, E. Fleming, G. Asuni, M. Jensen, F. Ur-Rehmann, and S. Pistorius, "Commissioning and validation of a novel measurement-based IMRT QA method, incorporating dose recalculation on patient CT data," Med. Phys. **35**(6), 2760–2760 (2008).
[24]B. E. Nelms, M. F. Chan, G. Jarry, M. Lemire, J. Lowden, C. Hampton, and V. Feygelman, "Evaluating IMRT and VMAT dose accuracy: Practical examples of failure to detect systematic errors when applying a commonly used metric and action levels," Med. Phys. **40**, 111722 (15pp.) (2013).
[25]P. F. Cadman, "Comment on 'IMRT commissioning: Some causes for concern'," Med. Phys. **38**(7), 4464–4465 (2011).
[26]M. Hussein, E. J. Adams, T. J. Jordan, C. H. Clark, and A. Nisbet, "A critical evaluation of the PTW 2D-array seven29 and OctaviusII phantom for IMRT and VMAT verification," J. Appl. Clin. Med. Phys. **14**(6), 274–292 (2013).
[27]D. A. Low, W. B. Harms, M. Sasa, and J. A. Purdy, "A technique for the quantitative evaluation of dose distributions," Med. Phys. **25**, 656–661 (1998).
[28]T. Depuydt, A. Van Esch, and D. P. Huyskens, "A quantitative evaluation of IMRT distributions: Refinement and clinical assessment of the gamma evaluation," Radiother. Oncol. **62**, 309–319 (2002).
[29]G. A. Ezzell *et al.*, "IMRT commissioning: Multiple institution planning and dosimetry comparisons, a report from AAPM Task Group 119," Med. Phys. **36**(11), 5359–5373 (2009).